Front. Med. 2021, 15(2): 302–312
https://doi.org/10.1007/s11684-021-0851-8

RESEARCH ARTICLE

DDB1- and CUL4-associated factor 8 plays a critical role in spermatogenesis

Xiuli Zhang[1,*], Zhizhou Xia[1,*], Xingyu Lv[2], Donghe Li[1], Mingzhu Liu[1], Ruihong Zhang[1], Tong Ji (✉)[3], Ping Liu (✉)[1], Ruibao Ren (✉)[1]

[1]*Shanghai Institute of Hematology, State Key Laboratory for Medical Genomics, National Research Center for Translational Medicine at Shanghai, Collaborative Innovation Center of Hematology, Ruijin Hospital Affiliated to Shanghai Jiao Tong University School of Medicine, Shanghai 200025, China;* [2]*Key Laboratory of Laparoscopic Technology of Zhejiang Province, Sir Run Run Shaw Hospital, Zhejiang University School of Medicine, Hangzhou 310058, China;* [3]*Department of General Surgery, Sir Run Run Shaw Hospital, Zhejiang University School of Medicine, Hangzhou 310058, China*

Abstract **Cullin-RING E3 ubiquitin ligase (CRL)-4 is a member of the large CRL family in eukaryotes. It plays important roles in a wide range of cellular processes, organismal development, and physiological and pathological conditions. DDB1- and CUL4-associated factor 8 (DCAF8) is a WD40 repeat-containing protein, which serves as a substrate receptor for CRL4. The physiological role of DCAF8 is unknown. In this study, we constructed *Dcaf8* knockout mice. Homozygous mice were viable with no noticeable abnormalities. However, the fertility of *Dcaf8*-deficient male mice was markedly impaired, consistent with the high expression of DCAF8 in adult mouse testis. Sperm movement characteristics, including progressive motility, path velocity, progressive velocity, and track speed, were significantly lower in *Dcaf8* knockout mice than in wild-type (WT) mice. However, the total motility was similar between WT and *Dcaf8* knockout sperm. More than 40% of spermatids in *Dcaf8* knockout mice showed pronounced morphological abnormalities with typical bent head malformation. The acrosome and nucleus of *Dcaf8* knockout sperm looked similar to those of WT sperm. *In vitro* tests showed that the fertilization rate of *Dcaf8* knockout mice was significantly reduced. The results demonstrated that DCAF8 plays a critical role in spermatogenesis, and DCAF8 is a key component of CRL4 function in the reproductive system.**

Keywords *Dcaf8*; male infertility; spermatogenesis

Introduction

Infertility is becoming a global emerging health problem; approximately 15% of couples suffer from fertility-related problems, and as many as 50% of cases can be attributed to male factors [1,2]. Three-quarters of these factors can be accounted for by aberrant spermatogenesis, a process divided into three phases: mitosis, meiosis, and spermiogenesis [3–6]. These special and complex processes demand spermatid-specific genes to execute their intricate roles, and an estimated 600–1000 germ cell-unique genes participate in spermiogenesis [7]. Disruption of the protein homeostasis required during spermatogenesis can lead to male infertility [8,9]. Thus, identifying the underlying pivotal genetic regulators of spermiogenesis may improve the diagnostic rate and clinical treatments for male infertility. Understanding the etiological factors of infertility and systematically identifying associated candidates is important.

Mainly regulated by the ubiquitin–proteasome system, proteolysis in germ cell meiosis and spermiogenesis is essential for virtually all steps of mammalian male gamete formation. A growing number of studies have verified that E3 ubiquitin ligase plays diverse and critical roles during spermatogenesis [10–13]. The Cullin-RING finger ligases (CRLs), which consist of one of seven Cullin protein scaffolds that interact with specific adaptors and various substrate receptors, are the largest family of ubiquitin

Received October 26, 2020; accepted February 20, 2021
Correspondence: Ruibao Ren, rbren@sjtu.edu.cn;
Ping Liu, liupingjize@126.com;
Tong Ji, jitong@zju.edu.cn

*These authors contributed equally to this study.

ligases in eukaryotes [14]. Previous studies have shown that CRL4 plays important roles in cell cycle progression, DNA damage response, DNA replication regulation, histone modification, hematopoiesis, and organismal development, as well as in pathogenesis of neuronal diseases and in tumorigenesis [15–19]. CRL4 can regulate the survival of both male and female germ cells [20]. The difference between CRL4 and other CRLs is that CRL4 employs WD40-like repeat-containing protein DDB1 (DNA damage binding protein 1) as linker protein. CRL4 substrate receptors that give substrate specificity to the appropriate CLR4 complex for ubiquitination are called DCAFs (DDB1-associated and Cullin-4-associated factors) [21,22].

Several CUL4-DDB1-DCAF components related to spermiogenesis have been studied in gene-targeted mouse models. One of the neddylation members of the Cullins, CUL4A, and its homolog, CUL4B, play distinct and vital roles during spermatogenesis [10,23–25]. CUL4A is specifically expressed during the meiosis stage of spermatocytes, and *Cul4a*-deficient male mice are infertile because of the defective meiotic progression of their gametes [10,25]. CUL4B is expressed in spermatogonia but predominantly in post-meiotic spermatids; male infertility resulting from *Cul4b* disruption has been attributed to abnormal post-meiotic sperm development [23,24]. *Dcaf17* knockout (KO) mice successfully represent the male infertility phenotype due to abnormal sperm development [26]. Here, we investigated the role of another CRL4 substrate adapter, DCAF8, on male fertility in mice.

DCAF8, also known as WDR42A, functions as a substrate recognition receptor for CUL4-DDB1 E3 ubiquitin ligase [22,27,28]. Histone H3 can be uniquely polyubiquitinated by $CRL4^{DCAF8}$ ubiquitin ligase to modify the fetal liver gene signature during liver maturation [29]. $CRL4^{DCAF8}$ regulates ubiquitination, degradation, and stabilization of MLF1 and MLF2, which play critical roles in hematopoiesis, leukemia, and various cancers [30]. The DCAF8 p.R317C mutation causes hereditary motor and sensory neuropathy with giant axons and mild cardiomyopathy [31]. The *Dcaf8* mRNA level was significantly upregulated in *Miwi* knockdown GC-2 cells, indicating that *Dcaf8* has a potential role in histone degradation during the pachytene stage of spermatogenesis [32,33]. However, the specific function of *Dcaf8* in spermatogenesis remains unknown.

In this study, we generated *Dcaf8* KO mice. We found that DCAF8 was predominantly expressed in adult mouse testis in the cytoplasm of spermatocytes but not in their nuclei. More than 40% of spermatids in *Dcaf8* KO male mice presented bent head malformations, and their fertilizing capability was impaired dramatically. These findings showed that *Dcaf8* plays an important role in spermatogenesis.

Materials and methods

Mice and genotyping

Dcaf8 KO mice were generated to introduce a myriad of mutations to exon 6 of the *Dcaf8* gene using CRISPR-Cas9 gene editing approaches. One founder mouse was found to harbor insertion of a fragment of 115 base pair nucleotides, which resulted in a frameshift in its coding sequence. Heterozygous mice were intercrossed to generate offspring with three different genotypes. Genomic DNA was isolated from mice toes using a genomic purification kit (Promega). Genotype validations were performed by PCR. Table 1 lists the primers used. The PCR conditions were as follows: 94 °C for 2 min, 35 cycles of 94 °C for 30 s, 60 °C for 45 s, 72 °C for 30 s, and a 10 min extension at 72 °C at the end of the run. PCR products were separated on 1.5% agarose gels; the wildtype (WT) and mutant alleles were 538 and 653 bp, respectively.

Analyses of mRNA expression

To detect the mRNA levels of *Dcaf8* in different mice tissues, we extracted total RNA using Trizol Reagent (Thermo Fisher) and quantified it using a Thermo Fisher Nano-Drop 2000c spectrophotometer. We took 500 ng of total RNA for reverse transcription using the Prime-Script RT Reagent kit (Takara). Real-time PCR was performed using cDNA products as templates from different tissues. Table 1 lists the primers used. *Dcaf8* expression levels were normalized to *Gapdh* by the $2^{-\Delta Ct}$ method and reported as fold changes [34].

Extraction of nuclear and cytoplasmic protein

After removing the tunica albuginea, the testes were digested to single cells using collagenase I (Thermo Fisher) and trypsin (Basal Media). The nuclear and cytoplasmic proteins were extracted according to a Nature Protocol publication [35]. In brief, the cells were lysed with hypotonic lysis buffer (10 mmol/L Tris HCl pH 8.0, 1 mmol/L KCl, 1.5 mmol/L $MgCl_2$, 1 mmol/L DTT, protease inhibitors, and ddH_2O) for 30 min, and the supernatant was collected as the cytoplasmic extract after centrifugation. The pellet was resuspended in NP-40 buffer (50 mmol/L Tris-HCl pH 8.0, 400 mmol/L NaCl, 5 mmol/L EDTA pH 8.0, 1% IGEPAL, 0.2% SDS, and ddH_2O) as the nuclear extract.

Western blot

The testes and cauda epididymis of mice were homogenized in liquid nitrogen and then lysed in 2× SDS lysis buffer (1 mol/L Tris buffer (pH 6.8), DTT, 10% SDS, glycerin, and ddH_2O). After three alternate 30 min cooling

Table 1 List of primers used in this study

Primer name	Primer sequence (5′–3′)	Purpose
Dcaf8-F	TCACATAGTAAGAGTGAGTGAAGC	*Dcaf8* KO mice genotyping
Dcaf8-R	CCCCATACAGACACTCATATACACA	*Dcaf8* KO mice genotyping
Gapdh-F	TGTGCAGTGCCAGCCTCGTC	RT-PCR
Gapdh-R	GCCACTGCAAATGGCAGCCC	RT-PCR
Dcaf8-F1	TTGACCTACCGGTTCTTCAGC	RT-PCR
Dcaf8-R1	TCTGTCGTGTTGGGACGTTT	RT-PCR

and boiling periods, we harvested the protein samples. On the basis of the molecular weight of the proteins, we subjected different concentrations of SDS-PAGE gels to electrophoresis and transferred the separated proteins to polyvinylidene fluoride membranes. We blocked the membranes with 5% nonfat milk for 1 h at room temperature and then incubated them with the special primary antibodies overnight at 4 °C. To visualize the protein bands, we incubated the membranes with labeled secondary antibody at room temperature for 1 h. Finally, proteins were detected with an ECL Plus kit. The primary antibodies used were anti-DCAF8 (Abcam), anti-Histone H3 (Abcam), and anti-GAPDH (Proteintech).

Male fertility test

Sexually mature male mice of two genotypes in WT groups ($n = 4$) and *Dcaf8* KO groups ($n = 16$) were mated with WT females at a 1:1 sex ratio for four continuous days, and the females were changed every day. Vaginal plugs were checked in the next morning every day. We counted the numbers of total females, plugged females, litters, and offspring in each group to calculate the frequencies of copulatory plug (FCP) and of conception (FC).

Sperm count

To evaluate epididymal sperm counts, the cauda epididymis from 10-week-old mice were dissected, placed into 1 mL of Hanks' balanced salt solution (HBSS), and maintained at 37 °C in a 5% CO_2 environment. Each epididymis was minced, allowing the sperm to swim out. After 20 min of incubation, we diluted the sperm suspensions for quantitative assessments.

Histology

To explore the progress of spermatogenesis, testes and epididymis were isolated from sexually mature 10-week-old mice with different genotypes. We directly fixed tissues in 4% paraformaldehyde overnight at 4 °C. Fixed tissues were rinsed with PBS and dehydrated in a series of 70%–100% ethanol solutions and embedded in paraffin. Sections (5 μm) were prepared on glass slides and stained with HE. The stained testis and epididymis sections were observed using an optical microscope to determine the different germ cell types during varying stages and the amounts of spermatozoa.

Immunofluorescence and immunohistochemical analyses

After treating the samples as described, we prepared slides for immunostaining of testis and epididymis. We hydrated and boiled the slides for 10 min in 0.1 mol/L sodium citrate using a microwave oven and cooled them in an ice box for antigen unmasking. We washed the slides three times for 5 min in PBS and blocked them in 10% goat serum for 1 h at room temperature. After blocking, the samples were triple-washed with PBS and incubated with anti-DCAF8 antibody (Abcam) overnight at 4 °C. Subsequently, the slides were triple-washed again in PBS and incubated with Alexa Fluor 555-conjugated goat anti-rabbit secondary antibody (CST) at room temperature for 1 h in a dark room. After a last PBS wash, we used Hoechst 33342 to dye the nuclei and Alexa Fluor 488-conjugated lectin peanut agglutinin (PNA) to label sperm acrosomes. For sperm immunofluorescence analyses, we dissected the cauda epididymis, and the sperm that swam out at 37 °C in HBSS were smeared onto slides. We entrusted the immunohistochemical staining to the Biossci Biotechnology Company. We observed all the samples at room temperature using a microscope.

Computer-assisted semen analysis (CASA)

Parameters of sperm motility were measured by CASA using an integrated visual optical system software (Hamilton-Thorne IVOSII). In brief, we dissected two sides of the cauda epididymis from each mouse (10 weeks old) and cut them once to allow sperm dispersion. We collected the sperm samples into 1.5 mL tubes containing 500 μL of modified Krebs–Ringer's bicarbonate solution (TYH medium) at 37 °C [36]. After 5 min of incubation, sperm were added to a counting chamber for analysis, and we examined five fields for each cauda epididymis. The instrument settings of CASA were as follows: temperature,

37 °C; minimum cell size, five pixels; minimum contrast, 50; minimum static contrast, 25; low VAP cutoff, 20.0; low VSL cutoff, 30.0; threshold straightness, 50%; static head size, 0.3–1.95; static head intensity, 0.5–1.3; and magnification, 0.89.

Transmission electron microscopy (TEM) and scanning electron microscopy (SEM)

TEM and SEM analyses were performed at the Laboratory of Electron Microscopy, Shanghai Jiao Tong University School of Medicine, following standard protocols [37]. In brief, testes were cut roughly into 1 mm cubes, and sperm isolated from cauda epididymis of both WT and *Dcaf8* KO mice were fixed in glutaraldehyde and osmium tetroxide (OsO_4). The specimens were then dehydrated in sucrose and embedded in epoxy resin. Ultrathin sections were prepared and picked up on nickel grids to be stained with uranyl acetate and methylcellulose. Finally, sections were observed under an electron microscope.

In vitro fertilization (IVF) assays

Female mice were injected with human chorionic gonadotropin, and the oocytes were collected after 14 h treatments and placed in human tubal fluid (HTF) medium covered with mineral oil. Sperm were freshly isolated from cauda epididymis of WT and *Dcaf8* KO mice and incubated in HTF medium at 37 °C under a 5% CO_2 environment for 1 h to allow capacitation. Oocytes were separated into two averaged pools and fertilized with sperm from either WT or *Dcaf8* KO mice individually. The percentages of 2-cell, 4-cell, and 8-cell embryos examined 24, 48, and 72 h later, respectively, were used as IVF rates.

Statistical analysis

All data from sperm counts, motility and IVF assays were analyzed using the GraphPad prism 7 software and presented as mean ± standard error of the mean. All the experiments were repeated at least three times. For each experiment, we used 3–7 animals. We performed two-tailed unpaired Student's *t*-tests and Chi-square test to compare the data and considered $P < 0.05$ as statistically significant.

Results

Expression patterns of *Dcaf8* in adult mice

We detected the tissue expression profiles of *Dcaf8* by RT-qPCR. We extracted RNA from 12 different tissues (brain, cauda epididymis, heart, liver, lung, ovary, kidney, spleen, adrenal gland, thymus, testis, and uterus). Fig. 1A shows the fold changes of *Dcaf8* mRNA level normalized to that of *Gapdh*. Among all the detected tissues, the testis exhibited the highest *Dcaf8* expression, suggesting that *Dcaf8* could be involved in spermatogenesis. The expression of DCAF8 in tissues was further verified by Western blot. The highest expression of DCAF8 protein was shown in the liver, while it ranked second in testicular expression (Fig. 1B). Using publicly available protein data from different species, we found that the WD40 repeat region of *Dcaf8* was highly conserved among human, monkey, mouse, rat, pig, and cattle DNA, further indicating that it may play an important biological function (Supplementary Table).

Generation of *Dcaf8* KO mice

The mouse *Dcaf8* gene includes 14 exons spanning approximately 7 kb. To investigate the function of *Dcaf8 in vivo*, *Dcaf8* KO mice were generated by inserting 115 bp nucleotides into exon 6 of *Dcaf8*, resulting in frameshifts of its coding sequence. The strategy was shown in Fig. 1C. The KO effect was verified by PCR analysis (Fig. 1D) and Western blots of testis and cauda epididymis tissues (Fig. 1E and 1F). Homozygous mice could be obtained by intercrossing heterozygous mice and were viable with no noticeable abnormalities. The total body weight was comparable with their WT littermates (Fig. 3A).

Male *Dcaf8* KO mice showed impaired fertility

To determine whether *Dcaf8* is associated with the reproduction process, we carried out breeding experiments where WT and *Dcaf8* KO mice were allowed to mate continuously with C57BL/6J females at a 1:1 ratio for 4 days. We found no differences in mating behavior between WT and *Dcaf8* KO mice by checking their ability to produce vaginal plugs in the female mice. The FCPs were 68.75% and 51.56% in WT and *Dcaf8* KO mice, respectively (Table 2). However, only 3 out of 33 WT females plugged by 16 *Dcaf8* KO males became pregnant and produced only 15 pups. In parallel, the 11 WT females plugged by 4 WT males produced 64 offspring pups in 9 litters (Table 2). Together, these data suggested that DCAF8 proteins were needed for male fertility, and the impaired fertility phenotype was not associated with abnormal sexual behavior.

Localization of DCAF8 in testis

As *Dcaf8* is expressed highly in testis, we performed immunofluorescence and immunohistochemistry experiments to investigate its distribution. We found that the DCAF8 protein was expressed in the cytoplasm of spermatocytes and almost absent in elongated sperm and mature sperm of adult mice. In addition, we confirmed the

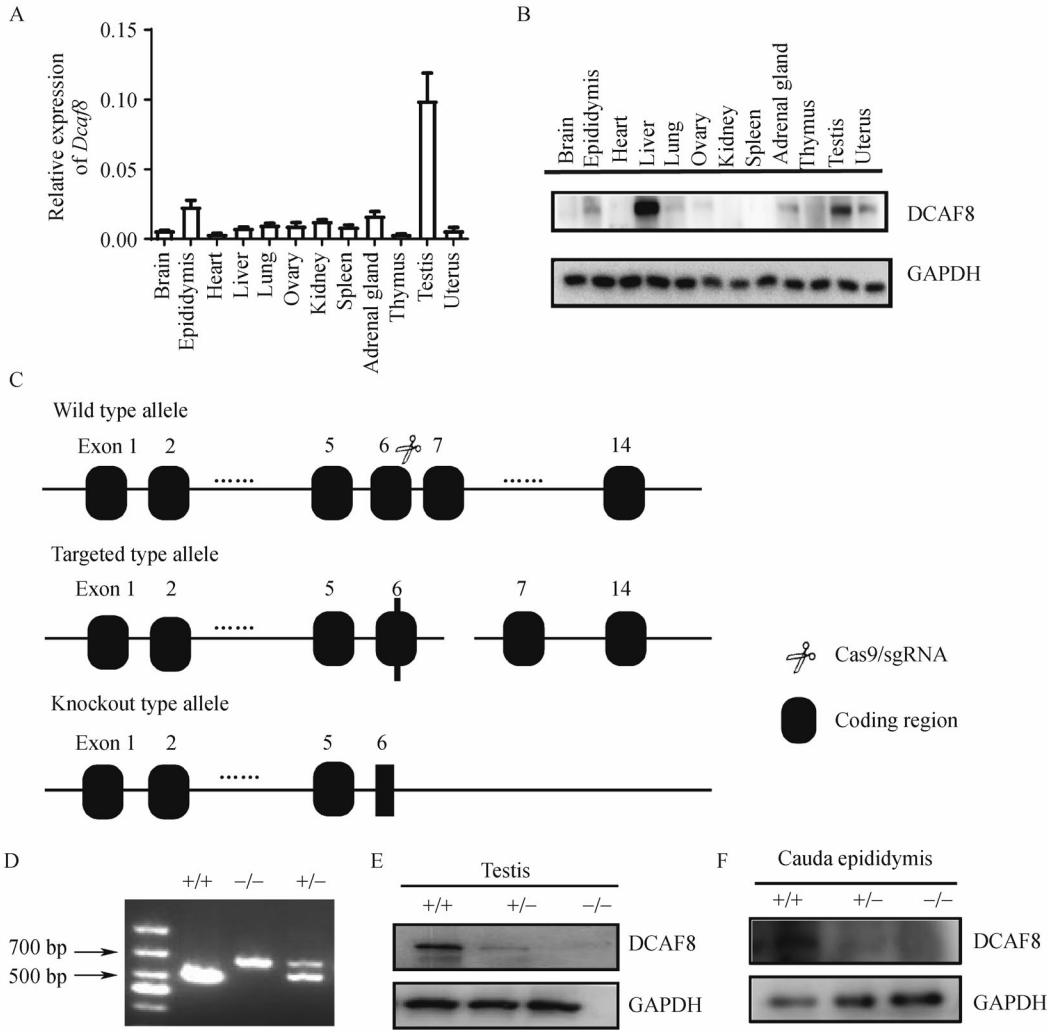

Fig. 1 *Dcaf8* expression among tissues and *Dcaf8* KO mice generation. (A) RT-PCR showing tissue expression profile of *Dcaf8* mRNA in adult mouse. (B) Expression of DCAF8 in different tissues of mice were immunoblotted. (C) The strategy for disruption of the *Dcaf8* gene of mouse. (D) Agarose gel image of three different *Dcaf8* genotypes. The expected size of PCR products (arrowheads) is shown on the left of the images. The band of WT product was 538 bp, while that of *Dcaf8* KO was 653 bp. (E and F) Western blot analysis showing the effect of *Dcaf8* KO in testis and epididymis. GAPDH was used as a loading control for total cellular proteins.

Table 2 Mating experiment of $Dcaf8^{+/+}$ and $Dcaf8^{-/-}$ mice

Male mice	Females	Plugs	Litters	Offspring	FCP (%)	FC (%)
$Dcaf8^{+/+}$ (n = 4)	16	11	9	64	68.75	81.82
$Dcaf8^{-/-}$(n = 16)	64	33	3	15	51.56	9.09

FCP, frequency of copulatory plug; FC, frequency of conception. FCP = (plugs/females) × 100%; FC = (litters/plugs) × 100%.
Results of statistical tests: FCP (P = 0.2684 NS), FC ($P < 0.001$, ***).

Dcaf8 KO effect (Fig. 2A–2D). To further verify the distribution pattern, we extracted cytoplasmic and nuclear proteins after testis digestion into single cells and found that DCAF8 showed cytoplasmic expression but was absent from nuclei (Fig. 2E). Such a unique expression pattern may indicate an essential physiologic role of *Dcaf8* during spermiogenesis in male mice.

Sperm counts and motility of *Dcaf8* KO male mice

To explore the mechanisms resulting in the impaired fertility of *Dcaf8*-deficient mice, we focused on the phenotypes of *Dcaf8* KO mice. The weights of testis and epididymis from sexually mature WT and *Dcaf8* KO mice were similar (Fig. 3B). We found no significant quantity

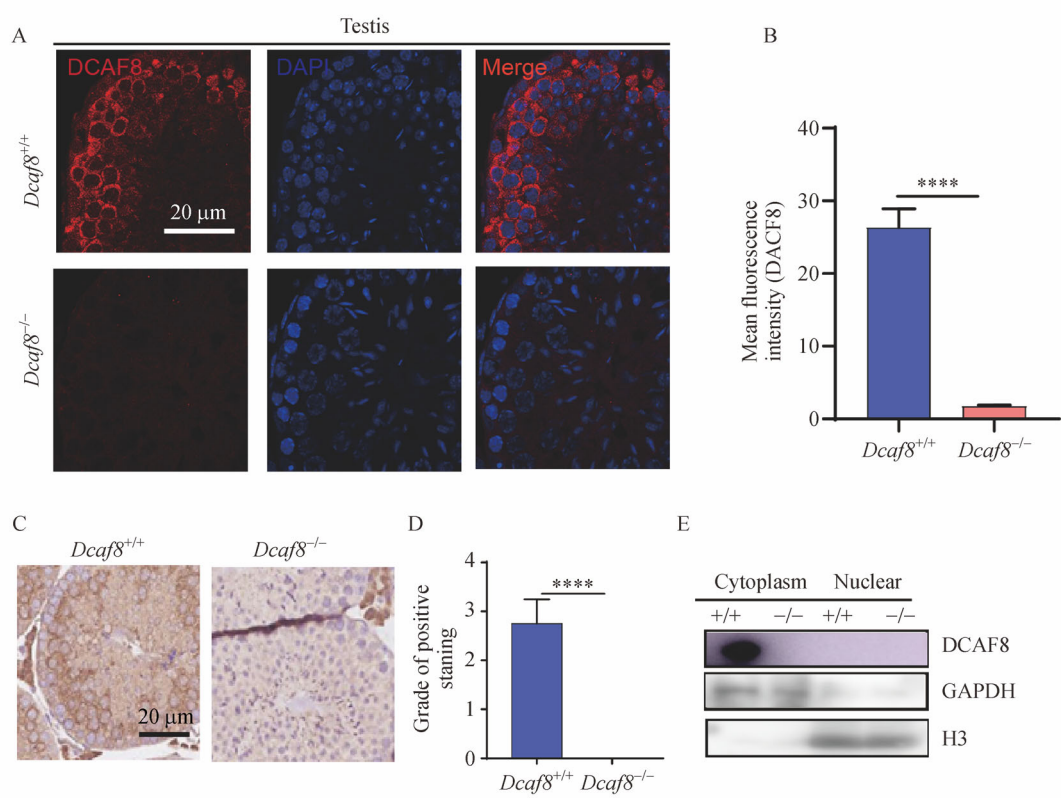

Fig. 2 Localization of DCAF8 in testis. (A and C) Immunofluorescence and immunohistochemistry assays revealing the localization of the DCAF8 protein in the adult mice testis. (B and D) Quantification of anti-DCAF8 staining density in (A) and (C). The mean fluorescence intensity of DCAF8 staining in (A) was calculated using ImageJ. In (C), fluorescent signaling abundance was calculated by staining intensity. Colorless was set as zero points, while light yellow as one point, brown and yellow for two points, and tan for three points. (E) Western blot of nuclear and cytoplasmic proteins further confirmed the localization of DCAF8. GAPDH and H3 served as the internal controls for cytoplasmic and nuclear proteins, respectively. (Two-tailed unpaired Student's *t*-test was used to compare the quantification of DCAF8 staining in Fig. 1A and 1C. **** $P < 0.0001$.)

differences in sperm production from the cauda epididymis between WT and *Dcaf8* KO mice (Fig. 3C and 3D). All these observations suggested that sperm production was unlikely to be associated with the impaired fertility of *Dcaf8* KO males. Moreover, we assessed the sperm motility activation after releasing sperm from the cauda epididymis by CASA. The movement characteristics including progressive motility, path velocity (VAP), progressive velocity (VSL), and track speed (VCL) were significantly lower in *Dcaf8* KO mice than in WT ones (Fig. 3E and 3F). However, total motility values were similar between WT and *Dcaf8* KO sperm (Fig. 3F).

Defective sperm morphology of *Dcaf8* KO mice

To examine sperm morphology of *Dcaf8* KO mice, we prepared sperm smears and stained them with Diff-Quick stain. The sperm from *Dcaf8* KO male mice showed higher percentages of bent head malformation than those of WT mice (data not shown). To understand the sperm defects in detail, we observed the sperm ultrastructure by SEM and TEM. Almost all the WT sperm were normal with a hook-shaped head, midpiece, and tail structures (Fig. 4A), whereas up to 40% of *Dcaf8* KO mice sperm exhibited bent head malformation (Fig. 4B), and the typical sperm head can be seen in Fig. 4C and 4D. To further analyze *Dcaf8* KO sperm defects, we stained WT and mutant sperm with PNA (green) and DAPI (blue), labeling the acrosomes and nuclei, respectively. No differences were observed between WT and *Dcaf8* KO sperm, and they all showed typical crescent-like acrosomes (green) covering the anterior portion of the head, even in the abnormal sperm of *Dcaf8* KO mice (Fig. 4E and 4G). Immunofluorescence showed that the number of spermatogenic cells were not influenced by *Dcaf8* KO (Fig. 4F). As mentioned above, the sperm bent head malformation may partially explain the impaired fertility of *Dcaf8* KO male mice.

Dcaf8 KO males showed severely reduced *in vitro* fertilization rates

We performed IVF assays to assess whether the fertility of *Dcaf8* KO sperm *in vitro* is disrupted or not. The two-cell stage embryos (24 h after sperm mixed with oocytes) of

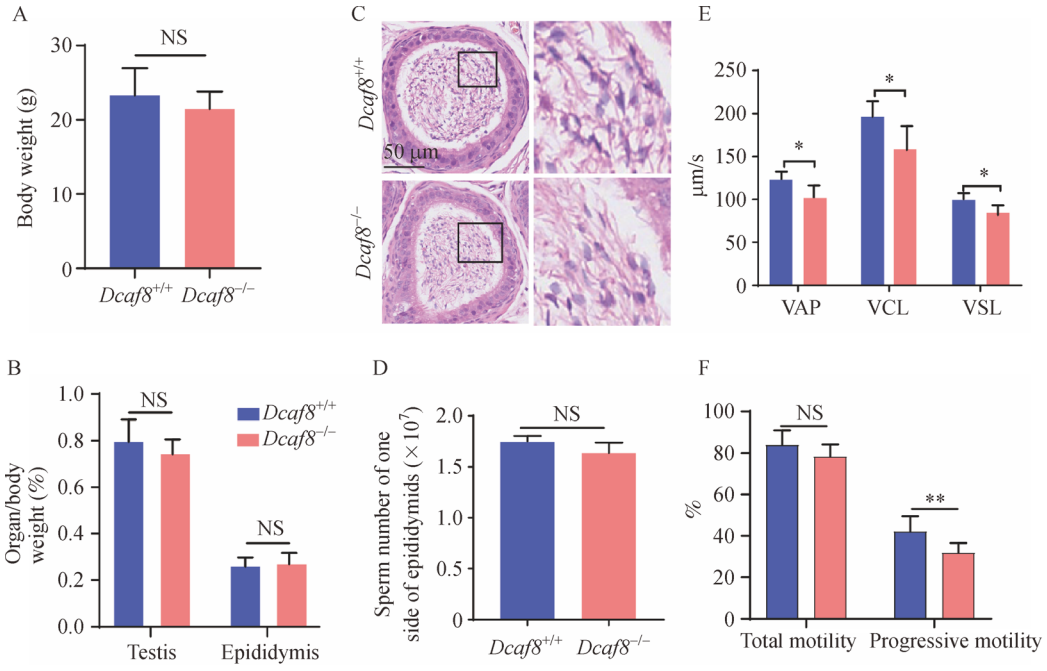

Fig. 3 Histology of the reproductive system, sperm count, and motilities of different genotypes. (A) Total body weight of WT and *Dcaf8* KO adult mice. (B) Assessing the testis and epididymis sizes of mice by calculating the ratio of testis or epididymis weight to body weight ($n = 7$ for WT and *Dcaf8* KO mice). (C and D) Sperm count analyses of WT and *Dcaf8* KO mice. (E and F) Sperm motility analyses of WT and *Dcaf8* KO mice. Five fields were observed for each replicate of sperm motility analysis. We used three pairs of mice to analyze sperm counts and four pairs of mice for motility. All the above studies were conducted with 10-week-old male mice. (NS, no significance; * $P < 0.05$, ** $P < 0.01$.)

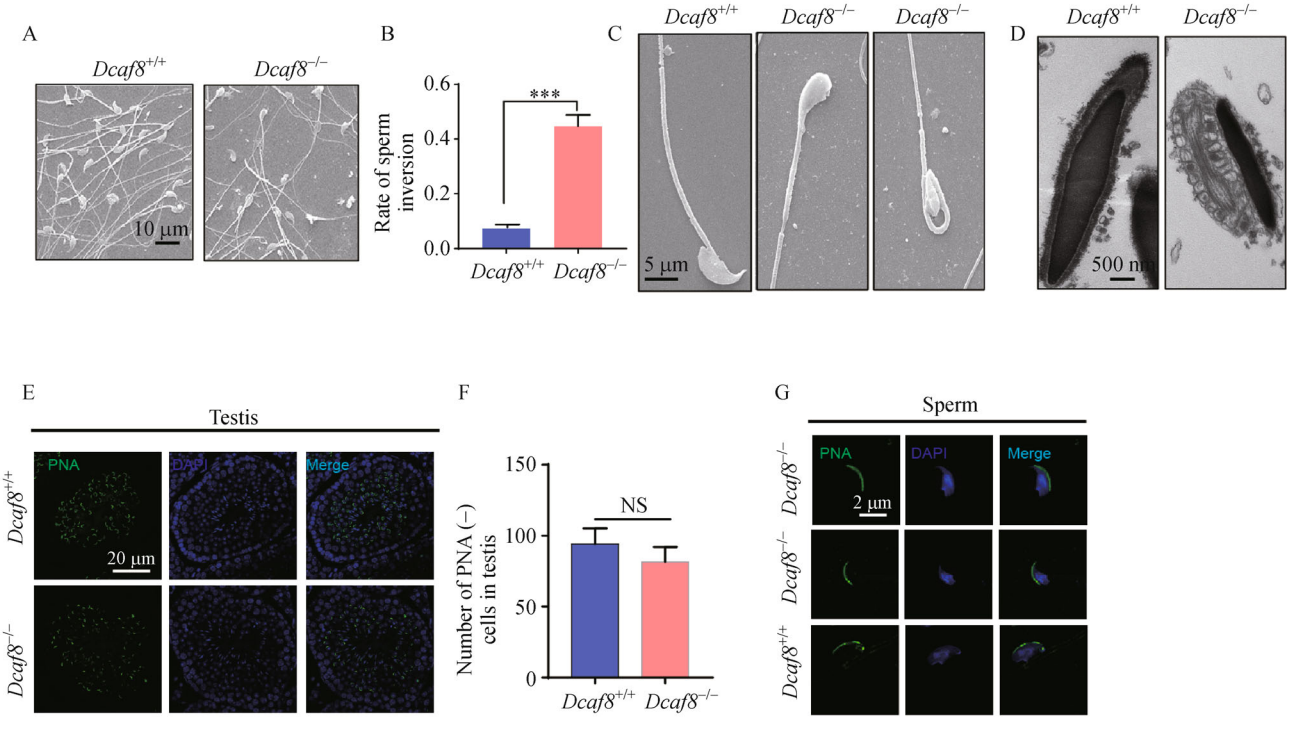

Fig. 4 Sperm morphology of *Dcaf8* KO mice. (A) Scanning electron microscopy (SEM) images of sperm from 10-week-old WT and *Dcaf8* KO mice observed under a microscope at a magnification of 1000×. (B) Statistical results of sperm head reflexes in three different visual fields of SEM. At least 100 sperms were included in each field. (C and D) SEM and transmission electron microscopy (TEM) micrographs of typical head reflexes of sperm in *Dcaf8* KO mice. (E,G) Confocal images of sperm from 10-week-old WT and *Dcaf8* KO mice co-stained with the acrosome marker PNA (green) and with DAPI (blue) under low- and high-power microscopy, respectively. (F) Statistical analysis of (E) to detect the number of PNA(−) cells in the testis of *Dcaf8* KO mice compared with that in the WT ones. (NS, no significance; *** $P < 0.001$.)

WT sperm appeared at a rate of approximately 60%, while those of *Dcaf8* KO sperm were dramatically fewer at a rate of approximately 8% (Fig. 5A). Furthermore, the 4-cell and 8-cell division stages were significantly better in *Dcaf8* WT mice than in the KO mice at 48 and 72 h, respectively (Fig. 5B and 5C). These results may explain the low *in vivo* fertilization rate of *Dcaf8* KO mice shown in Table 2. These findings suggested that the *Dcaf8* KO male mice's inability to reproduce could be explained by their low *in vivo* migration ability and *in vitro* sperm–egg binding ability.

Discussion

Mammalian male fertilization is a complex event for which success depends on multiple steps, including the generation of spermatozoa carrying intact genomes and capability of fusion with the egg. Various factors have been reported to be essential for fertilization in studies targeting mice genes [38,39]. However, many specific genes with crucial roles during fertilization still need to be uncovered to provide guidance on diagnosis and treatments for male patients.

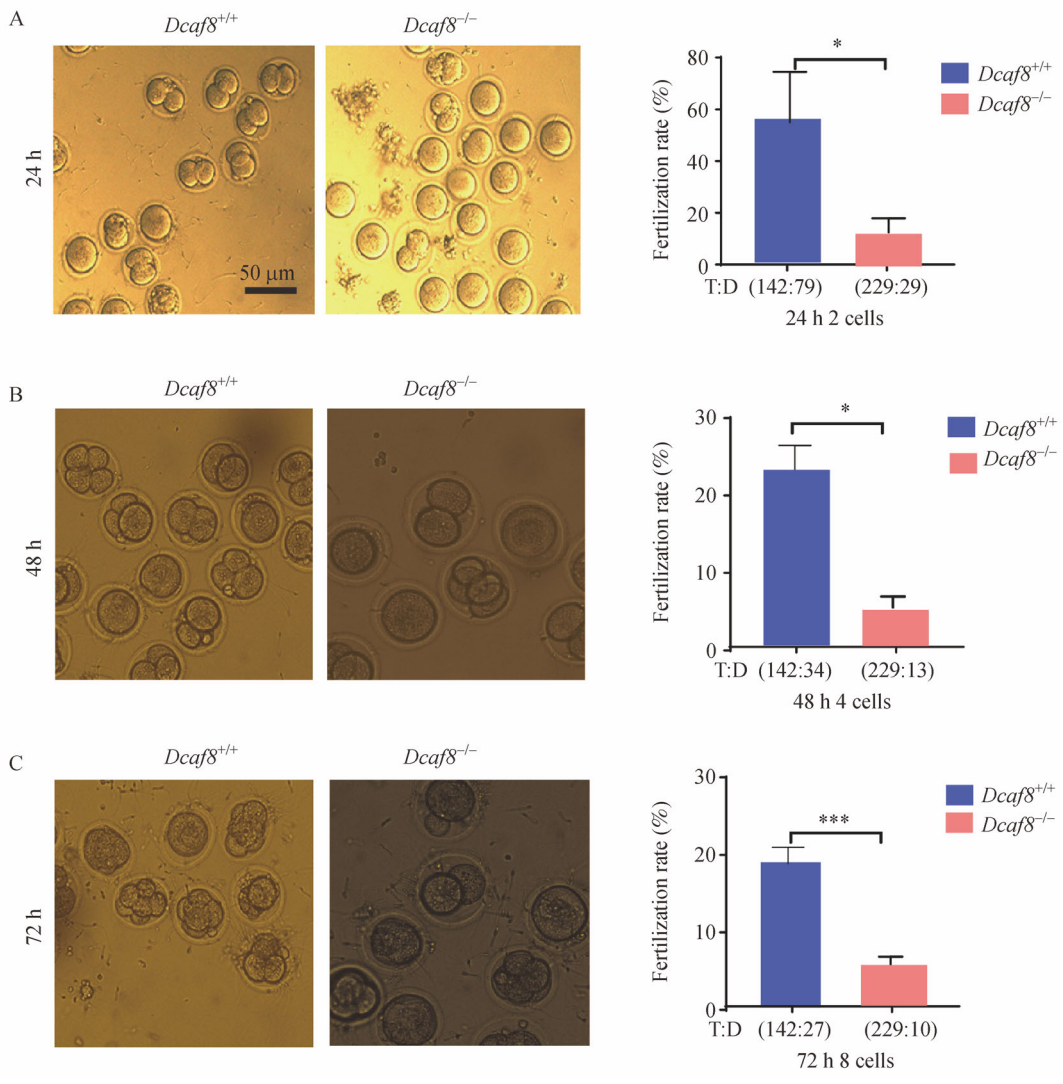

Fig. 5 Inability of *Dcaf8* KO sperm to fertilize eggs *in vitro*. (A–C) The eggs obtained from super-ovulation female mice were incubated with capacitated WT or *Dcaf8* KO sperm *in vitro*. *Dcaf8* KO sperm showed severely deficient oocyte binding. The IVF rate was dramatically lower in samples from *Dcaf8* KO male mice than in those from WT mice. The average of total cells and division cells counted was shown in graphics. Graphics A, B, and C represent the ratio of total oocytes developed to a 2-cell, 4-cell, and 8-cell stage, respectively. T, total cells counted; D, division cells counted at different stages. (*$P < 0.05$, ***$P < 0.001$.)

Many E3 ubiquitin ligases are essential for spermatogenesis regulation from spermatogonia to mature sperm stages [40,41]. Many of the genes involved are expressed at high rates and/or uniquely in the testis, including *Cul4a, Cul4b,* and *Dcaf17* [10,24,26,42]. Studies have shown that deletion of *Ddb1,* which is associated with both *Cul4a* and *Cul4b*, leads to defects in oocyte survival, oocyte meiotic maturation, and post-meiotic oocyte maintenance [43–45]. These findings suggested that the CRL4 E3 ubiquitin complex is indispensable during germ cell development. In this study, we revealed that DCAF8, a previously uncharacterized E3 ubiquitin ligase substrate adapter, plays an important role during male fertilization, and the fertility of male mice deficient in *Dcaf8* is significantly impaired.

Interestingly, the *Dcaf8* sequence is highly conserved among several species. On the basis of the predominant expression of *Dcaf8* mRNA levels in testis shown in our study, *Dcaf8* may play an essential testicular function role. Mice with *Dcaf8* deficiency displayed normal embryonic development without clear anatomical abnormalities. We verified the impaired fertility of *Dcaf8* male KO mice using mating tests as shown in Table 2. Our results showed that the frequency of conception after mating with WT male mice was 81.82%, while that after mating with *Dcaf8* KO mice decreased to 9.09%. However, the FCP were similar between these two groups, implying that the *Dcaf8*-deficient male mice displayed normal sexuality. Studies have revealed that *Cul4a* KO mice testis was twofold smaller in size and weight compared with WT testis [10]. However, *Dcaf8* KO mice had no effects on the size or weight of their testis in our study. The normal mating behavior of our *Dcaf8* KO mice and their apparently normal anatomical structures suggested that the impaired infertility was not related to aberrant reproductive physiology, sex organ development, or sexual behavior.

To achieve successful fertilization, enough sperm need to be deposited into the female reproductive tract; sperm with normal morphology, vigorous motility, and sound fertilizing capabilities are necessary [46,47]. To uncover the mechanisms leading to impaired fertility of the *Dcaf8* KO male mice, we assessed all the variables mentioned above. However, the amount of sperm produced by the *Dcaf8* KO mice was similar to that of their WT littermates. Moreover, CASA analysis revealed similar total motilities between the two genotypes, while the *Dcaf8* KO mice showed just slightly lower progressive motility, VAP, VSL, and VCL than the WT mice. We observed aberrant sperm morphology under SEM and TEM with almost half of the spermatids exhibiting bent head malformation. This specific malformation may have adverse effects on the fertilization rate. In addition, the reduced fertilization rate was verified by IVF experiments. To a considerable degree, the impaired fertility phenotype in *Dcaf8* KO male mice was caused by the sperm's defective morphology and attenuated motility. The subfertility phenotype observed in *Dcaf8* KO male mice demonstrated vital functions of DCAF8 proteins during spermatogenesis. DCAF8 is a member of DCAF family proteins; it serves as a substrate receptor that provides substrate specificity to ubiquitin for CRL4 E3 ligase complexes. Spermatogenesis is affected in *Cul4A*, *Cul4B, Dcaf17*, and *Dcaf8* KO mice [10,24,26], and *Dcaf1* and *Dcaf13* KO mice show vital functions in maintaining mammalian oogenesis [44,48]. One can reasonably assume that the CRL4 E3 ligase complexes may be involved in the regulation of the reproductive system via degrading certain proteins through ubiquitination, and the insights observed may also be applicable to humans. However, these assumptions need to be explored by further investigation.

In the study, we used *Dcaf8*-deficient mice to demonstrate the significant role of *Dcaf8* in male fertility. Even though DCAF8 is exclusively expressed in spermatocytes and is nearly vanished in mature sperm, it was found to participate in sperm motility and morphogenetics. Further dissecting this functional network will enhance our understanding of this E3 ligase complex component during spermiogenesis.

Acknowledgements

This work was supported by the Key Program of Natural Science Foundation of China (Nos. 8153006 and 81870112 to Ruibao Ren, No. 81970134 to Ping Liu), Shanghai Science and Technology Development Funds (No. 18ZR1423600 to Ruibao Ren), Shanghai Collaborative Innovation Program on Regenerative Medicine and Stem Cell Research (No. 2019CXJQ01 to Ruibao Ren), the Samuel Waxman Cancer Research Foundation and Innovative Research Team of High-level Local Universities in Shanghai (to Ruibao Ren).

Compliance with ethics guidelines

Xiuli Zhang, Zhizhou Xia, Xingyu Lv, Donghe Li, Mingzhu Liu, Ruihong Zhang, Tong Ji, Ping Liu, and Ruibao Ren declare that they have no conflicts of interest. All institutional and national guidelines for the care and use of laboratory animals were followed.

Electronic Supplementary Material Supplementary material is available in the online version of this article at https://doi.org/10.1007/s11684-021-0851-8 and is accessible for authorized users.

References

1. Neto FT, Bach PV, Najari BB, Li PS, Goldstein M. Genetics of male infertility. Curr Urol Rep 2016; 17(10): 70
2. Schlegel PN. Evaluation of male infertility. Minerva Ginecol 2009; 61(4): 261–283

3. O'Flynn O'Brien KL, Varghese AC, Agarwal A. The genetic causes of male factor infertility: a review. Fertil Steril 2010; 93(1): 1–12
4. Krausz C. Male infertility: pathogenesis and clinical diagnosis. Best Pract Res Clin Endocrinol Metab 2011; 25(2): 271–285
5. Eddy EM. Male germ cell gene expression. Recent Prog Horm Res 2002; 57(1): 103–128
6. de Kretser DM, Loveland KL, Meinhardt A, Simorangkir D, Wreford N. Spermatogenesis. Hum Reprod 1998; 13(Suppl 1): 1–8
7. Schultz N, Hamra FK, Garbers DL. A multitude of genes expressed solely in meiotic or postmeiotic spermatogenic cells offers a myriad of contraceptive targets. Proc Natl Acad Sci USA 2003; 100(21): 12201–12206
8. Hou CC, Yang WX. New insights to the ubiquitin-proteasome pathway (UPP) mechanism during spermatogenesis. Mol Biol Rep 2013; 40(4): 3213–3230
9. Baarends WM, van der Laan R, Grootegoed JA. Specific aspects of the ubiquitin system in spermatogenesis. J Endocrinol Invest 2000; 23(9): 597–604
10. Kopanja D, Roy N, Stoyanova T, Hess RA, Bagchi S, Raychaudhuri P. Cul4A is essential for spermatogenesis and male fertility. Dev Biol 2011; 352(2): 278–287
11. Ma T, Keller JA, Yu X. RNF8-dependent histone ubiquitination during DNA damage response and spermatogenesis. Acta Biochim Biophys Sin (Shanghai) 2011; 43(5): 339–345
12. Wang S, Zheng H, Esaki Y, Kelly F, Yan W. Cullin3 is a KLHL10-interacting protein preferentially expressed during late spermiogenesis. Biol Reprod 2006; 74(1): 102–108
13. Lu LY, Wu J, Ye L, Gavrilina GB, Saunders TL, Yu X. RNF8-dependent histone modifications regulate nucleosome removal during spermatogenesis. Dev Cell 2010; 18(3): 371–384
14. Petroski MD, Deshaies RJ. Function and regulation of Cullin-RING ubiquitin ligases. Nat Rev Mol Cell Biol 2005; 6(1): 9–20
15. Jackson S, Xiong Y. CRL4s: the CUL4-RING E3 ubiquitin ligases. Trends Biochem Sci 2009; 34(11): 562–570
16. O'Connell BC, Harper JW. Ubiquitin proteasome system (UPS): what can chromatin do for you? Curr Opin Cell Biol 2007; 19(2): 206–214
17. Zhong W, Feng H, Santiago FE, Kipreos ET. CUL-4 ubiquitin ligase maintains genome stability by restraining DNA-replication licensing. Nature 2003; 423(6942): 885–889
18. Sugasawa K. The CUL4 enigma: culling DNA repair factors. Mol Cell 2009; 34(4): 403–404
19. Cheng J, Guo J, North BJ, Tao K, Zhou P, Wei W. The emerging role for Cullin 4 family of E3 ligases in tumorigenesis. Biochim Biophys Acta Rev Cancer 2019; 1871(1): 138–159
20. Wang H, Zhai L, Xu J, Joo HY, Jackson S, Erdjument-Bromage H, Tempst P, Xiong Y, Zhang Y. Histone H3 and H4 ubiquitylation by the CUL4-DDB-ROC1 ubiquitin ligase facilitates cellular response to DNA damage. Mol Cell 2006; 22(3): 383–394
21. Lee J, Zhou P. DCAFs, the missing link of the CUL4-DDB1 ubiquitin ligase. Mol Cell 2007; 26(6): 775–780
22. Angers S, Li T, Yi X, MacCoss MJ, Moon RT, Zheng N. Molecular architecture and assembly of the DDB1-CUL4A ubiquitin ligase machinery. Nature 2006; 443(7111): 590–593
23. Yin Y, Liu L, Yang C, Lin C, Veith GM, Wang C, Sutovsky P, Zhou P, Ma L. Cell autonomous and nonautonomous function of CUL4B in mouse spermatogenesis. J Biol Chem 2016; 291(13): 6923–6935
24. Lin CY, Chen CY, Yu CH, Yu IS, Lin SR, Wu JT, Lin YH, Kuo PL, Wu JC, Lin SW. Human X-linked intellectual disability factor CUL4B is required for post-meiotic sperm development and male fertility. Sci Rep 2016; 6(1): 20227
25. Yin Y, Lin C, Kim ST, Roig I, Chen H, Liu L, Veith GM, Jin RU, Keeney S, Jasin M, Moley K, Zhou P, Ma L. The E3 ubiquitin ligase Cullin 4A regulates meiotic progression in mouse spermatogenesis. Dev Biol 2011; 356(1): 51–62
26. Ali A, Mistry BV, Ahmed HA, Abdulla R, Amer HA, Prince A, Alazami AM, Alkuraya FS, Assiri A. Deletion of DDB1- and CUL4-associated factor-17 (Dcaf17) gene causes spermatogenesis defects and male infertility in mice. Sci Rep 2018; 8(1): 9202
27. Wu Y, Zhou L, Wang X, Lu J, Zhang R, Liang X, Wang L, Deng W, Zeng YX, Huang H, Kang T. A genome-scale CRISPR-Cas9 screening method for protein stability reveals novel regulators of Cdc25A. Cell Discov 2016; 2(1): 16014
28. Nowak M, Suenkel B, Porras P, Migotti R, Schmidt F, Kny M, Zhu X, Wanker EE, Dittmar G, Fielitz J, Sommer T. DCAF8, a novel MuRF1 interaction partner, promotes muscle atrophy. J Cell Sci 2019; 132(17): jcs233395
29. Li G, Ji T, Chen J, Fu Y, Hou L, Feng Y, Zhang T, Song T, Zhao J, Endo Y, Lin H, Cai X, Cang Y. $CRL4^{DCAF8}$ ubiquitin ligase targets histone H3K79 and promotes H3K9 methylation in the liver. Cell Rep 2017; 18(6): 1499–1511
30. Huang D, Liu C, Sun X, Sun X, Qu Y, Tang Y, Li G, Tong T. $CRL4^{DCAF8}$ and USP11 oppositely regulate the stability of myeloid leukemia factors (MLFs). Biochem Biophys Res Commun 2020; 529(2): 127–132
31. Klein CJ, Wu Y, Vogel P, Goebel HH, Bönnemann C, Zukosky K, Botuyan MV, Duan X, Middha S, Atkinson EJ, Mer G, Dyck PJ. Ubiquitin ligase defect by DCAF8 mutation causes HMSN2 with giant axons. Neurology 2014; 82(10): 873–878
32. Gou LT, Dai P, Yang JH, Xue Y, Hu YP, Zhou Y, Kang JY, Wang X, Li H, Hua MM, Zhao S, Hu SD, Wu LG, Shi HJ, Li Y, Fu XD, Qu LH, Wang ED, Liu MF. Pachytene piRNAs instruct massive mRNA elimination during late spermiogenesis. Cell Res 2015; 25 (2): 266
33. Gou LT, Kang JY, Dai P, Wang X, Li F, Zhao S, Zhang M, Hua MM, Lu Y, Zhu Y, Li Z, Chen H, Wu LG, Li D, Fu XD, Li J, Shi HJ, Liu MF. Ubiquitination-deficient mutations in human Piwi cause male infertility by impairing histone-to-protamine exchange during spermiogenesis. Cell 2017; 169(6):1090–1104.e13
34. Livak KJ, Schmittgen TD. Analysis of relative gene expression data using real-time quantitative PCR and the $2(-\Delta\Delta C(T))$ method. Methods 2001; 25(4): 402–408
35. Shechter D, Dormann HL, Allis CD, Hake SB. Extraction, purification and analysis of histones. Nat Protoc 2007; 2(6): 1445–1457
36. Quinn P, Kerin JF, Warnes GM. Improved pregnancy rate in human *in vitro* fertilization with the use of a medium based on the composition of human tubal fluid. Fertil Steril 1985; 44(4): 493–498
37. Chen Q, Peng H, Lei L, Zhang Y, Kuang H, Cao Y, Shi QX, Ma T, Duan E. Aquaporin3 is a sperm water channel essential for postcopulatory sperm osmoadaptation and migration. Cell Res 2011; 21(6): 922–933
38. Matzuk MM, Lamb DJ. Genetic dissection of mammalian fertility pathways. Nat Cell Biol 2002; 4(Suppl): s41–s49

39. Jamsai D, O'Bryan MK. Mouse models in male fertility research. Asian J Androl 2011; 13(1): 139–151
40. Sutovsky P. Ubiquitin-dependent proteolysis in mammalian spermatogenesis, fertilization, and sperm quality control: killing three birds with one stone. Microsc Res Tech 2003; 61(1): 88–102
41. Kanatsu-Shinohara M, Onoyama I, Nakayama KI, Shinohara T. Skp1-Cullin-F-box (SCF)-type ubiquitin ligase FBXW7 negatively regulates spermatogonial stem cell self-renewal. Proc Natl Acad Sci USA 2014; 111(24): 8826–8831
42. Hou X, Zhang W, Xiao Z, Gan H, Lin X, Liao S, Han C. Mining and characterization of ubiquitin E3 ligases expressed in the mouse testis. BMC Genomics 2012; 13(1): 495
43. Yu C, Zhang YL, Pan WW, Li XM, Wang ZW, Ge ZJ, Zhou JJ, Cang Y, Tong C, Sun QY, Fan HY. CRL4 complex regulates mammalian oocyte survival and reprogramming by activation of TET proteins. Science 2013; 342(6165): 1518–1521
44. Yu C, Xu YW, Sha QQ, Fan HY. CRL4DCAF1 is required in activated oocytes for follicle maintenance and ovulation. Mol Hum Reprod 2015; 21(2): 195–205
45. Yu C, Ji SY, Sha QQ, Sun QY, Fan HY. CRL4-DCAF1 ubiquitin E3 ligase directs protein phosphatase 2A degradation to control oocyte meiotic maturation. Nat Commun 2015; 6(1): 8017
46. Suarez SS, Pacey AA. Sperm transport in the female reproductive tract. Hum Reprod Update 2006; 12(1): 23–37
47. Sutton KA, Jungnickel MK, Florman HM. A polycystin-1 controls postcopulatory reproductive selection in mice. Proc Natl Acad Sci USA 2008; 105(25): 8661–8666
48. Zhang J, Zhang YL, Zhao LW, Guo JX, Yu JL, Ji SY, Cao LR, Zhang SY, Shen L, Ou XH, Fan HY. Mammalian nucleolar protein DCAF13 is essential for ovarian follicle maintenance and oocyte growth by mediating rRNA processing. Cell Death Differ 2019; 26 (7): 1251–1266